

# Thermo-fluid dynamics of woody biomass flue gas in the heat accumulation stoves

**Paolo Scotton – University of Padova, Padova, Italy**

**Daniele Rossi – University of Padova, Padova, Italy**

**Mauro Barberi – Barberi Stufe LTD, Trento Italy**

**Stefano De Toni – Barberi Stufe LTD, Trento Italy**

## Abstract

The research aims to clarify some aspects of the thermo-fluid dynamics of woody biomass flue gas within the refractory twisted conduit inside heat accumulation stoves. These are traditional heating elements in the European Alpine regions, whose history began in the fifteenth century. The high temperature flue gas flows in a twisted conduit, releasing heat along its path to the refractory. The heat stored in the refractory is then released slowly into the environment mainly as a radiant component. The physical phenomena that occur in an accumulation stove, once the activation energy in the combustion chamber has been provided, continues, initially increasing temperature and velocity of flue gases and then decreasing the two variables until the end of the reaction. The decreasing temperatures of flue gases, flowing from the combustion chamber in the twisted conduit, tends to cause the transition of the flow regime from laminar to turbulent conditions [1] [2]. Moreover the continuous changes of direction imposed by the curves cause local contractions and expansions of the flux and, consequently, energy losses which are difficult to evaluate. The way the heat transfer occurs appears to depend mainly on gas flow conditions (laminar or turbulent) and on the radiative properties of the hot particle cloud inside the flue gas. The physical properties of the conduit (roughness of the internal surface), as well as the thermodynamic properties of the refractory material (its mass and its geometric arrangement), play a fundamental role in the functionality of the stove. This paper describes some analysis performed on heat transport and exchange processes inside the flue gases and between them and the refractory. The importance of the radiation properties of the flue gasses has been highlighted. The numerical results, obtained with

COMSOL® Non Isothermal Flow ( $k-\epsilon$  turbulent model), have been compared with laboratory measures.

## 1. Introduction

The research regards some thermo-fluid dynamic aspects of the biomass flue gas of a particular kind of heat accumulation stove made of ceramic and refractory. They consist of a combustion chamber,



Fig. 1 – View of a project design of a modern stove, where the combustion chamber and twisted conduit are visible and a phase of its construction (Barberi Ltd).

where woody material is burned, followed by a twisted conduit where the flue gases transfer heat to the refractory.

Due to the heat transfer along the pipe, the kinematic viscosity of the flue gas decreases, the density increases and the Reynolds number increases causing transition from laminar to turbulent motion. Moreover the continuous changes of direction imposed by the curves cause local contractions and expansions of the flux and, consequently, energy losses that are difficult to evaluate. The stored heat is released slowly in the rooms of the house mainly in the form of radiant heat from the ceramic tiles of the external surface.

The way the heat transfer happens depends mainly on gas flow conditions (laminar or turbulent) and on the radiative properties of the hot particle cloud inside the flue gas. From this point of view, the composition of flue gas plays a fundamental role in the global behaviour of the heat transfer. The physical properties of the conduit (shape, roughness of the internal surface), as well as the thermodynamic properties of the refractory material, its mass and its geometric arrangement, are other main aspects of the stove's functionality. The representation of the phenomena described above is the goal of the present research, in order to provide increased awareness in the design process of these technological elements, which is strongly affected by the uncertainties described above.

Working in that direction, some physical models have been realized by the laboratory of Barberi Ltd, on which several measures of temperature, pressure and velocity have been taken, both inside the gases and on the outer surface of the conduit.

In the present paper we show the numerical results obtained reproducing one geometrically simplified physical model, under unsteady flow regime. All the numerical applications have been performed on the basis of previous experiences reported in [1], [2] and [4].

## 2. Physical Model

For a simplified analysis of the behaviour of the heat accumulation stove a physical model has been

built. It was realized in blocks of refractory material (normally used for the construction of the stoves) and it is described below.

### 2.1 Geometry and materials

The physical model is composed by a combustion chamber (height 0.89 m, width 0.81 m, depth 0.70 m), a straight refractory conduit (length 6.0 m, inner diameter 180.0 mm) and a chimney (Fig. 2). The combustion chamber has been connected to the refractory conduit by means of a black steel pipe.

The conduit lies on a continuous support made of calcespan. The air, necessary for the combustion reactions, was supplied by a natural draught. It was introduced into the combustion chamber through an instrumented stainless steel pipe where a valve, a diaphragm and a thermocouple were installed. The mass flow of the flue gas was deduced from the mass flow of the air supply, according to EN 15544 [5].

In Table the thermo-technical characteristics of the materials are reported.

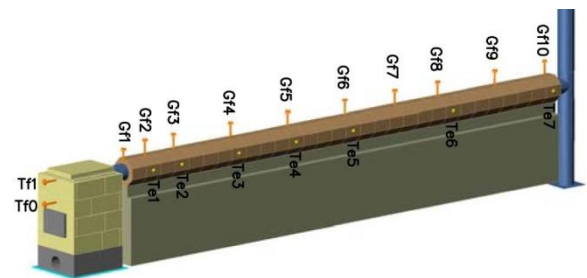


Fig. 2 – The simplified configuration of a heat accumulation stove built for the study of its behaviour (Barberi Ltd).

	refract.	calcespan	steel
$\rho$	2550 [kg/m <sup>3</sup> ]	600 [kg/m <sup>3</sup> ]	7990 [kg/m <sup>3</sup> ]
$C_p$	859 [J/kg K]	1000 [J/kg K]	500 [J/kg K]
$k$	3.16 [W/m K]	0.15 [W/m K]	50 [W/m K]
$\varepsilon$	0.95 [-]	0.70 [-]	0.95 [-]

Table 1: Thermo-technical properties of the materials (Barberi Ltd).

### 2.2 Experimental measures

The measurements of temperature inside the flue gas have been taken at the middle point of ten sections of the pipe ( $G_f$ ) by K – thermocouples. The temperatures at the outer surface are taken at 7 positions as indicated in Fig. 2 ( $T_e$ ). Three

temperature measurements of the surrounding atmosphere have been taken: one above and two on the lateral side of the refractory conduit. The radiant heat of one side of the conduit was caught by means of an infrared camera, in order to obtain another temperature estimation.

The physical phenomena that occur in an accumulation stove, once the activation energy in the combustion chamber has been provided, continue, initially increasing temperature and velocity of flue gases and then decreasing the two variables until the end of the reaction. This causes a continuous variation in the motion conditions at the inlet of refractory conduit (Table 2). In addition, due to the heat transfer along the pipe, the gas kinematic viscosity decreases whereas the density increases, causing the increase of the Reynolds number.

The variability in time of some parameters, estimated at the *Gf1* thermocouple (Fig. 2), are shown in Fig. 3 and Table 2.

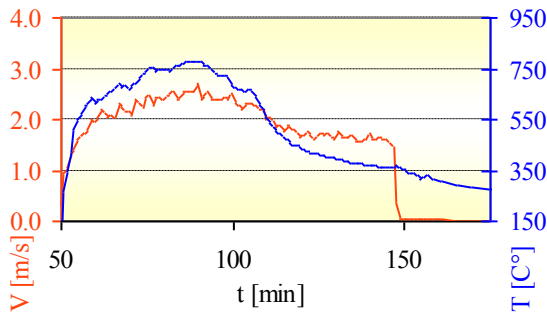


Fig. 3 – Measured temperature and calculated velocity at the inlet of refractory conduit.

### 3. Mathematical model

The set of physical and chemical processes taking place inside the combustion chamber and inside the flue gas conduit are very complex and, currently, not yet completely understood.

t [min.]	$T_{Gf1}$ [°C]	$\rho$ [kg/m <sup>3</sup> ]	V [m/s]	Re [-]	$h_{PL}$ [mm]
50.0	14.95	1.186	0.30	4079	12.5
51.4	347.02	0.551	1.04	3578	14.2
53.8	510.13	0.436	1.42	3301	15.1
55.8	570.66	0.405	1.70	3509	14.3
60.7	628.91	0.379	2.04	3795	13.3
67.7	671.90	0.361	2.28	3951	12.9
75.8	755.86	0.332	2.46	3760	13.4
82.8	751.50	0.333	2.53	3891	13.0
88.7	776.83	0.325	2.55	3787	13.4
92.7	759.41	0.331	2.55	3878	13.1
99.7	686.94	0.356	2.46	4163	12.3
108.7	584.74	0.398	2.18	4384	11.7
117.7	449.48	0.473	1.82	4827	10.7
126.8	408.22	0.501	1.68	4914	10.5
139.8	366.65	0.534	1.67	5433	9.6
146.8	362.53	0.537	1.44	4737	10.9
147.8	366.74	0.534	0.36	1171	41.1
147.9	360.75	0.539	0.04	132	—

Table 2 – Temperatures surveyed from *Gf1* thermocouple, calculated density [5], velocity and Reynolds number of flue gas and, in the last column, the thickness required (by the software Comsol [7]) for the first cells of the boundary layer.

In the present work we have focused our attention on fluid dynamics and thermal processes inside the flue gas conduit.

#### 3.1 Governing equations

The Navier – Stokes equations describe the motion of viscous fluids. For a single-phase flow they are composed by the continuity equation:

$$\frac{\partial \rho}{\partial t} + \nabla \cdot (\rho \vec{u}) = 0, \quad (1)$$

and by the momentum equation:

$$\rho \frac{\partial \vec{u}}{\partial t} + \rho \vec{u} \cdot \nabla \vec{u} = -\nabla p + \nabla \cdot \tau + F, \quad (2)$$

where the viscous stress tensor is given by

$$\tau = \mu \left( \nabla \vec{u} + \nabla \vec{u}^T \right) - \frac{2}{3} \mu \left( \nabla \cdot \vec{u} \right) \vec{I}.$$

For turbulent flows the Navier – Stokes equations are simplified, through the average over the time, in the Reynolds – Averaged Navier Stokes (RANS) equations [6] [7].

In the term  $F$ , to the right hand of (2), are present also the buoyancy forces  $F = -\rho g$ , responsible for

the flow stratification and for the natural draught of the stove. The density  $\rho$  is, however, a variable of the problem and depends on the temperature. Therefore, the buoyancy forces can be introduced in the momentum equations through the first Boussinesq approximation:

$$F = -(\rho - \rho_R)g \quad (3)$$

or with the second order of approximation:

$$F = -\rho_R \beta (T - T_R)g \quad (4)$$

For both Boussinesq approximations the associated boundary condition is  $dp/dy = 0$ .

The heat transfer in one physic system is provided by conduction, convection and radiation. For conduction in a multidimensional isotropic system, the Fourier law can be rewritten in the form ([8] [10]):

$$q = -k \nabla T \quad (5)$$

The convection heat transfer, which occurs between a wall at temperature  $T_w$  and the surrounding atmosphere at undisturbed temperature  $T_\infty$  ([8] [10]), can be represented by

the equation:

$$q = h(T_w - T_\infty). \quad (6)$$

where  $h = Nu \cdot k / d$ .

In the study of the heat transfer by radiation, in the cases where heat is supplied to the physical system by combustion of any fuel type, the flue gas has to be considered as a participant medium. It is composed of a fraction of molecular gas and a part of particulate matter. Its interaction with the radiative intensity travelling in a given direction ( $I(\Omega_i)$ ) occurs through absorption, emission and scattering [10].

The radiation absorption of the particulate matter has been observed to be proportional to the magnitude of the incident energy as well as the distance the beam travels ( $s$ ) through the medium:

$$\frac{dI_{abs}}{ds} = -\kappa I(\Omega; s). \quad (7)$$

At the given temperature  $T$ , the rate of emission from a volume element will be equivalent to a fraction of emission intensity of the black body:

$$\frac{dI_{em}}{ds} = \kappa I_b(T). \quad (8)$$

The scattering can be distinguished in out-scattering and in-scattering. The out-scattering

considers the part of incoming intensity that is deviated from the considered direction of propagation (9). The out-scattering intensity appears, therefore, as augmentation energy (in-scattering) along another direction.

$$\frac{dI_{out-sc}}{ds} = -\sigma_s I(\Omega; s) \quad (9)$$

The in-scattering has contributions from all directions and, therefore, must be calculated by integration over all solid angles  $\Omega_i$ :

$$\frac{dI_{in-sc}}{ds} = -\sigma_s / (4\pi) \int_{4\pi} I(\Omega_i) \phi(\Omega_i; \Omega) d\Omega_i \quad (10)$$

Considering the two terms of attenuation, absorption and out-scattering, leads to define the extinction coefficient through the path  $s$ :

$$\frac{dI_{extinction}}{ds} = -\beta I(\Omega; s), \quad (11)$$

where  $\beta = \kappa + \sigma_s$  is the extinction coefficient.

The equation of heat transfer by radiation (Radiation Transfer Equation - RTE), in the direction of solid angle ( $\Omega \cdot \nabla I(\Omega)$ ) reads [9] [10]:

$$\kappa I_b(T) - \beta I(\Omega; s) - \frac{\sigma_s}{4\pi} \int_{4\pi} I(\Omega_i) \phi(\Omega_i; \Omega) d\Omega_i. \quad (12)$$

Another component of heat transfer by radiation occurs between the outer surface, at temperature  $T_w$ , and the surrounding ambient at undisturbed temperature  $T_\infty$ . This component of heat exchange can be written as:

$$q = \varepsilon \sigma (T_\infty^4 - T_w^4) \quad (13)$$

### 3.2 Model settings

The first set of simulations was carried out on the part of experimental apparatus that goes from the steel conduit, required to connect the heater to the refractory conduit, to the control section located in the chimney, 2.7 m above the floor. The flue gas was considered radiatively a transparent medium. The boundary conditions for the unsteady problem are the pressure at the final section and mass discharge (calculated using the literature equations reported in EN 15544 [5]) at the initial section. In these numerical models the buoyancy forces have been considered using the first Boussinesq approximation (3).

On the outer surface, a boundary condition of convective cooling (6) was used together with a

boundary condition for the radiation from surface to the ambient (13).

	Complete model (M1) no radiation	partial model (M2) yes radiation
$h_{FL}$	0.36 [mm]	—
$h_{Tr}$	2.9 [mm]	14.4 [mm]
$h_{Te}$	29.1 [mm]	480.0 [mm]
N° El.	$139.1 \cdot 10^3$	$9.8 \cdot 10^3$
D.O.F.	$175.5 \cdot 10^3$	$114.5 \cdot 10^3$

Table 3 – Thickness of the first layer of boundary layer  $h_{FL}$ ; minimum height of triangular cells  $h_{Tr}$  and tetrahedral cells  $h_{Te}$ , total number of mesh elements N° El.; degrees of freedom of the system for the two configurations.

The numerical results of temperature were significantly different from the measured ones. So, it was supposed that the heat transfer by radiation of the flue gas could not be neglected.

In order to investigate the effects of the radiation with participant media, a second set of simulations were made.

Because of the slowness of the numerical research of the solution of these problems, a reduced geometry, first four meters, with a coarse mesh was considered.

The Radiation Transfer Equation – RTE (12), introduced into the numerical model, was solved using the method of Discrete – Ordinate Approximation with the  $S_2$  discretization [9] [10]. The values of absorption and scattering used are respectively equal to 0.8307 [1/m] and 0.0 [1/m].

It was decided to use the k- $\epsilon$  model [6]. The characteristics of the meshes are shown in Table 3.

The characteristics of the workstation are two Intel® Xeon® CPU X5550, 2.67 GHz (eight processors) and 24GB ram with a 64 bit software.

### 3.3 Results and discussion

The average cross-sectional values of velocity, pressure and temperature along the conduit were evaluated (Fig. 4). The data were calculated at the 88th minute, corresponding to the peak time of the temperature (Fig. 3). The average velocity of the flue gas is well approximated by a segment of straight line with a mean-square deviation (R2) equal to 0.95.

The average temperature distribution can be well represented by an exponential function. The mean-square deviation, in this case, was equal to 0.99.

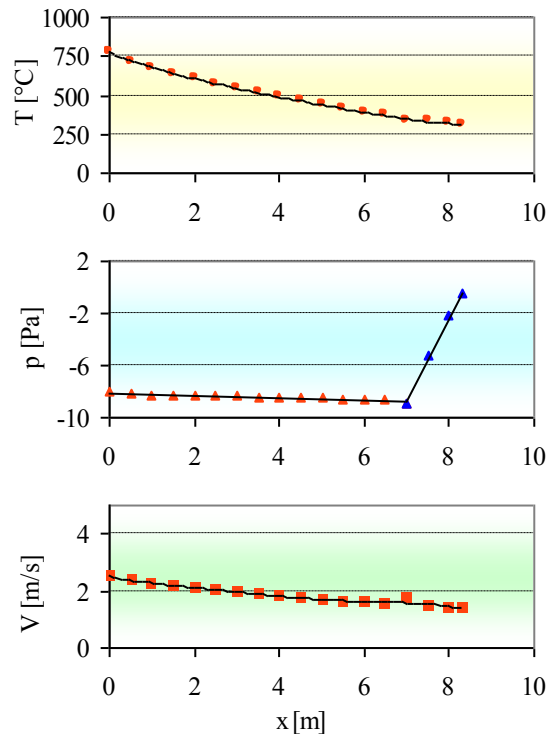


Fig. 4 – Longitudinal evolution of the mean cross-sectional values (temperature, pressure, velocity) at the 88th minute.

As far as the pressure is concerned, a more complex reasoning should be made. In the horizontal refractory pipe, the pressure values decrease gradually until the sharp curve, used as a connection between the horizontal section and the chimney. Then the trend starts to grow again to reach the undisturbed pressure value of the outlet cross section.

This pressure trend is caused by buoyancy forces (3). Previous results of numerical simulations showed that if those forces were neglected, it was not possible to obtain this behaviour [3]. In general, the average pressure pattern can be well approximated by a segment of straight line, both for the first horizontal section (mean-square deviation equal to 0.89) and for the vertical chimney section (mean-square deviation equal to 1.00).

In Fig. 5 the temperature values, measured and calculated, obtained from the first numerical model (M1), considering the flue gas as a transparent

medium are compared at three cross-sections. At the first section, the temperature of the flue gas measured and calculated in the middle of the conduit are in quite good agreement (Gf3), especially after the instant of the maximum temperature. This is not the same, however, for the outer surface (Te2). At the other two sections the behaviour tends to be the opposite. The interruption of the combustion air supply, after 150 minutes, produces numerical results quite different from the measured ones, mainly at the first section. An explanation for that has not yet been reached by the authors. The point could be investigated by analysing the effect of the mesh discretization, of the heat transfer coefficients and also of the system's thermal capacity, including the thermal capacity of the flue gas.

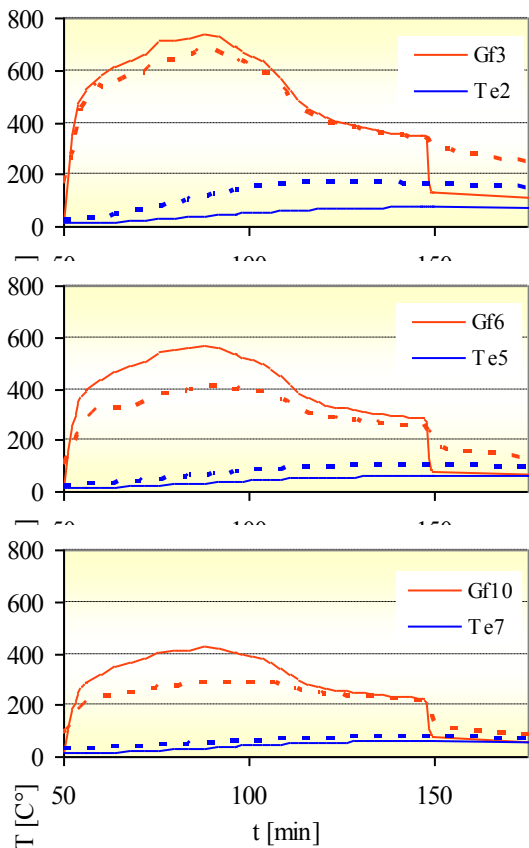


Fig. 5 – Temperatures measured on a physical model (dotted line) and calculated from a numerical model (solid line) at three cross-sections.

Due to the high temperatures of the phenomenon, it is reasonable to give radiation an important role. So, we introduced the radiative transfer equation into the model.

The length of the numerical apparatus has been limited to four meters because of the large increase of equations to solve. The value 0.831 has been given to the absorption coefficient  $\kappa$ , and the value 1.073 has been given to the scattering coefficient  $\sigma_s$ , ([9]).

The agreement between the calculated and measured temperature was significantly improved, especially in the first meters of the model, in the time period during which the model kept the numerical stability.

At the Gf3 thermocouple, the numerical results are superimposed on those measured. At the Gf6 thermocouple the numerical results are closer to the physical data but not yet satisfactory (Fig. 6). The behaviour of the temperatures calculated on the outer surface of the pipe (not shown in Fig. 6) does not differ significantly from the one calculated with the first numerical model (Fig. 5).

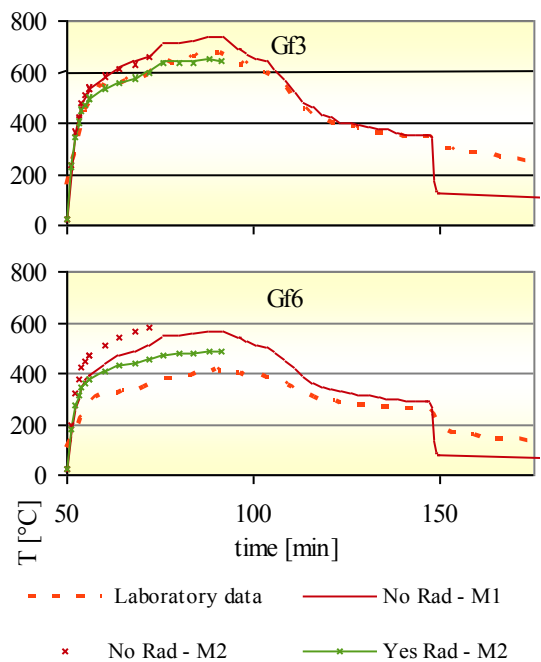


Fig. 6 – Temperatures experimentally measured and numerically calculated with the first (M1, Table 2) and the second (M2, Table 2) numerical model at the Gf3 and Gf6 thermocouples (Fig. 2).

In order to cover the gap between physical and numerical data, we are working on a better definition of the radiative parameters of the flue gas, on the thermal characteristics of the refractory material, which have been considered, until now, independent of temperature, and on the boundary conditions posed on the outer surface of the conduit.

## 4. Conclusions

Even if the numerical applications show significant differences from the laboratory data, we think we are going in the right direction to simulate this challenging thermo-fluid-dynamic process.

There should be at least three main reasons for the differences.

The first one is related to the reliability of the experimental measurements. The very difficult experimental conditions (very high temperatures, very low pressures) induce to accept high errors of the order of 15%-20%.

The second one is of a numerical type. The choice of the mesh significantly influences the numerical solution [4]. In particular, near a wall, the choice of the mesh could have great influence on the heat transfer through the wall. Some calculations based on the numerical results of the liminar coefficients have produced values that seem to be three or four times lower than the physical ones.

The third reason is the capability of taking account of all the physical processes which are present in the real phenomenon. Problems arise both from the physical interpretation of the phenomena and from the capability of the software to positively complete the numerical simulation. In the present simulations, for instance, we have seen the importance of the radiation absorption and emission phenomena of particle fraction of the flue gas [9]. At the same time we needed to limit the numerical integration in time because of numerical instabilities.

The research is currently devoted to a deeper understanding of the role of the different radiative terms of the flue gas and to their appropriate definition in our case.

## 5. Acknowledgement

The research has been financed by the Trentino (Italy) Provincial law n. 6, 1999, call 2008 - project: "La stufa ad accumulo-Innovazione nella tradizione" of the Barberi Ltd.

## 6. Nomenclature

### Symbols

$d$	diameter	[m]
$h$	convective coefficient	[W/(m <sup>2</sup> K)]
$h_{FL}$	thickness of the first layer of boundary layer	[mm]
$h_{Tr}$	minimum height of triangular cells	[mm]
$h_{Te}$	minimum height of tetrahedral cells	[mm]
$k$	thermal conductivity	[W/(m K)]
$\kappa$	absorption coefficient	[1/m]
$\bar{I}$	identity matrix	[-]
$I$	radiative intensity	[-]
$I_b$	black body radiative intensity	[-]
$\mu$	dynamic viscosity	[Pa]
$Nu$	Nusselt number	[-]
$\Omega_i$	solid angle in $i$ direction	[sr]
$p$	Pressure	[Pa]
$q$	heat flux	[W/m <sup>2</sup> ]
$\rho$	density	[kg/m <sup>3</sup> ]
$\rho_R$	reference density	[kg/m <sup>3</sup> ]
$s$	beam travel distance	[m]
$\sigma_s$	scattering coefficient	[1/m]
$t$	time	[s]
$T$	temperature	[°C]
$T_w$	wall temperature	[°C]
$T_\infty$	undisturbed temperature	[°C]
$T_R$	reference temperature	[°C]
$\tau$	viscous stress tensor	[Pa]
$\vec{u}$	velocity vector	[m/s]

## References

- [1] Scotton P., Rossi D. 2011, Studio della dinamica del moto dei fumi nelle stufe ad accumulo – Relazione 1° anno, (2011), prot. n. 442 (2010), Department of Geosciences, Univ. of Padova;
- [2] Scotton P., Rossi D. 2011, Study of Gas Dynamics in the Heat-accumulation Stoves, Comsol Conference 2011 Stuttgart Proceedings, ISBN 978-0-9839688-0-1;
- [3] Scotton P., Rossi D. 2012, Studio della dinamica del moto dei fumi nelle stufe ad accumulo – Relazione 2° anno, (2012), prot. n. 442 (2010), Department of Geosciences, Univ. of Padova;
- [4] Scotton P. Rossi D., Barberi M., De Toni S. 2012, Thermo-Fluid Dynamics of Flue Gas in Heat Accumulation Stoves: Study Cases, Comsol Conference 2012 Boston Proceedings, ISBN 978-0-9839688-8-7;
- [5] EN-15544, One of kachelgrundöfen putzgrundöfen (tiled mortared stoves) – calculation method;
- [6] Garde R. J. 2010, Turbulent Flow, New Age International, 2010.
- [7] Comsol Multiphysics, CFD Module User's Guid;
- [8] Faghri A., Zhang Y., Howel J. 2010, Advanced Heat and Mass Transfer, Global Digital Press, Columbia, USA;
- [9] Modest M. F. 1993, Radiative Heat Transfer, McGraw Hill;
- [10] Comsol Multiphysics, Heat Transfer Module User's Guid;